Inflammatory Bowel Diseases, 2023, **29**, 444–457
https://doi.org/10.1093/ibd/izac219
Advance access publication 26 October 2022
Original Research Articles - Basic Science

Colonic Epithelial Circadian Disruption Worsens Dextran Sulfate Sodium–Induced Colitis

Sarah B. Jochum, MD,[*] Phillip A. Engen, MS,[†] Maliha Shaikh, MS,[†] Ankur Naqib, PhD,[†] Sherry Wilber,[†] Shohreh Raeisi, MS,[†] Lijuan Zhang, MD,[†] Shiwen Song, MD,[‡] Gabriella Sanzo, BA,[†] Vijit Chouhan, MD,[†] Frank Ko, PhD,[§] Zoe Post, MD,[†,¶] Laura Tran, BS,[†] Vivian Ramirez, MS,[†] Stefan J. Green, PhD,[‖] Khashayarsha Khazaie, PhD,[**] Dana M. Hayden, MD, MPH,[††] Mark J. Brown, PhD,[‡‡] Robin M. Voigt, PhD,[†,¶] Christopher B. Forsyth, PhD,[†,¶] Ali Keshavarzian, MD,[†,¶,§§] and Garth R. Swanson, MD, MS[†,¶]

From the [*]Department of Surgery, Rush University Medical Center, Chicago, IL, USA;
[†]Rush Center for Integrated Microbiome and Chronobiology Research, Rush Medical College, Rush University Medical Center, Chicago, IL, USA;
[‡]Department of Pathology, GoPath Global Pathology Service, Buffalo Grove, IL, USA;
[§]Department of Cell and Molecular Medicine, Rush University Medical Center, Chicago, IL, USA;
[¶]Department of Medicine, Rush University Medical Center, Chicago, IL, USA;
[‖]Genomics and Microbiome Core Facility, Rush University Medical Center, Chicago, IL, USA;
[**]Department of Immunology, Mayo Clinic College of Medicine, Rochester, MN, USA;
[††]Division of Colon and Rectal Surgery, Department of Surgery, Rush University Medical Center, Chicago, IL, USA;
[‡‡]Department of Cellular and Molecular Medicine, Cleveland Clinic, Cleveland, OH, USA; and
[§§]Department of Physiology, Rush University Medical Center, Chicago, IL, USA.

Address correspondence to: Dr. Garth R. Swanson, MD, MS, Rush University Medical Center, 1725 West Harrison Street, Suite 206, Chicago, IL 60612, USA (garth_swanson@rush.edu).

Background: Disruption of central circadian rhythms likely mediated by changes in microbiota and a decrease in gut-derived metabolites like short chain fatty acids (SCFAs) negatively impacts colonic barrier homeostasis. We aimed to explore the effects of isolated peripheral colonic circadian disruption on the colonic barrier in a mouse model of colitis and explore the mechanisms, including intestinal microbiota community structure and function.

Methods: Colon epithelial cell circadian rhythms were conditionally genetically disrupted in mice: TS4Cre-BMAL1lox (cBMAL1KO) with TS4Cre as control animals. Colitis was induced through 5 days of 2% dextran sulfate sodium (DSS). Disease activity index and intestinal barrier were assessed, as were fecal microbiota and metabolites.

Results: Colitis symptoms were worse in mice with peripheral circadian disruption (cBMAL1KO). Specifically, the disease activity index and intestinal permeability were significantly higher in circadian-disrupted mice compared with control animals (TS4Cre) ($P < .05$). The worsening of colitis appears to be mediated, in part, through JAK (Janus kinase)-mediated STAT3 (signal transducer and activator of transcription 3), which was significantly elevated in circadian-disrupted (cBMAL1KO) mice treated with DSS ($P < .05$). Circadian-disrupted (cBMAL1KO) mice also had decreased SCFA metabolite concentrations and decreased relative abundances of SCFA-producing bacteria in their stool when compared with control animals (TS4Cre).

Conclusions: Disruption of intestinal circadian rhythms in colonic epithelial cells promoted more severe colitis, increased inflammatory mediators (STAT3 [signal transducer and activator of transcription 3]), and decreased gut microbiota–derived SCFAs compared with DSS alone. Further investigation elucidating the molecular mechanisms behind these findings could provide novel circadian directed targets and strategies in the treatment of inflammatory bowel disease.

Lay Summary

Disruption of peripheral circadian rhythms of the colon epithelium results in worse colitis and increased intestinal permeability in mice when given dextran sulfate sodium. This may be mediated through alterations in microbiota, butyrate levels, and STAT3.

Keywords: circadian disruption, ulcerative colitis, peripheral circadian disruption, microbiota, metabolomics.

Introduction

Inflammatory bowel disease (IBD) is a debilitating chronic relapsing and remitting condition of the gastrointestinal tract. IBD has a highly variable disease course characterized by episodes of flare that can result in hospitalizations, surgery, chronic steroid use, and decreased quality of life.[1] Identifying risk factors for exacerbations is essential to decrease morbidity and healthcare burdens for IBD patients. One such

Received for publication: November 16, 2021. Editorial Decision: September 20, 2022

Key Messages

The master circadian clock in the brain (central) regulates multiple peripheral circadian clocks including those in the gastrointestinal tract; disruption of central circadian clock has been shown to worsen colitis.

This study demonstrates that disruption of the peripheral circadian clock machinery in the colonic epithelial cells, with normal central circadian timing, results in increased colitis, mortality, intestinal permeability, inflammation, and dysbiosis.

This study highlights the importance of studying environmental factors that impact circadian timing in inflammatory bowel disease including both central (sleep-wake cycle) and peripheral (meal timing), as both may impact colitis.

risk factor is central circadian rhythm disruption, which has been identified as a potential risk factor for a more severe IBD course.[2] Central circadian rhythms regulate nearly every aspect of biology and behavior including immune system activity and metabolism.[3] The master or central circadian clock is located in the superchiasmatic nucleus. This master clock influences peripheral circadian clocks, which are located in nearly every cell of the body, including in the intestinal epithelial cells (IECs) of the gastrointestinal tract.[4] On the molecular level, the core circadian clock comprises a transcriptional and translational feedback loop of core clock proteins, including BMAL1 and BMAL2, cryptochrome 1 and 2, period 1 to 3, REV-ERBα/b, retinoic acid-related orphan receptor α, and CLOCK,[4] which cycle in a pattern that takes approximately 24 hours to complete.

These circadian rhythms are sensitive to changes in the environment. For example, bright light is the main regulator of the central circadian clock, whereas time of food consumption robustly regulates circadian rhythms in the intestine. A mismatch (ie, misalignment) between the endogenous circadian clock and the external environment can be detrimental to health. Light at the wrong time can disrupt the central circadian clock, and late-night eating (ie, wrong-time eating) can disrupt circadian rhythms in the intestine.[5] Recently, peripheral circadian misalignment due to wrong-time eating has been found to increase metabolic syndrome, worsen glucose control in diabetics, and increase risk of colon cancer.[6-8]

Disruption of central circadian rhythms has been studied in IBD using several animal models including both environmental (altering light-dark cycles),[9,10] and genetic (manipulation of the core molecular clock, eg, global knockout of REV-ERBα) approaches.[11] These studies find that central circadian disruption is associated with more severe dextran sulfate sodium (DSS)–induced colitis. However, the consequences of disrupted peripheral circadian rhythm of the colon in an IBD model have not yet been adequately investigated.

IEC barrier disruption is the primary driver of DSS-induced colitis. Multiple studies have suggested that central circadian rhythm disruption promotes colitis through IEC barrier changes: (1) studies by our group and others demonstrate that expressions of tight junction proteins are under circadian control, resulting in diurnal fluctuations in IEC apical junction complex (AJC) protein expression and intestinal barrier function in mice; (2) disruption of the intestinal microbiota community (dysbiosis) with decreased relative abundance of the short-chain fatty acid (SCFA)–producing bacteria is associated with epithelial barrier dysfunction; and (3) key molecules that are pivotal for activation of the intestinal inflammatory cascade in the intestine, such as signal transducer and activator of transcription protein 3 (STAT3), are under circadian control,[12] and circadian disruption leads to elevated phospho-STAT3 in colon IECs, which is associated with worse colitis.[13]

Therefore, we hypothesized that colon-specific peripheral circadian rhythm disruption worsens colitis through disruption of IEC barrier integrity. To test this hypothesis, we took advantage of an IEC-specific knockout mouse model to determine whether genetic disruption of IEC circadian rhythm machinery worsens DSS-induced colitis. TS4Cre (Fabp1Cre) is expressed in mature differentiated enterocytes (IECs) of the colon and distal ileum.[14] Thus, TS4Cre-BMAL1^{lox} (cBMAL1KO) mice are a model of peripheral circadian rhythm disruption in the colon while the central circadian rhythm remains intact. This study explores the impact of isolated peripheral circadian disruption of the colon IECs in a rodent colitis model and elucidates potential key mediators in STAT3 and the SCFA-producing bacteria in which peripheral circadian rhythm disruption induced worsening of colitis.

Methods

Murine Experimental Model

TS4Cre and BMAL1lox mice, generously provided from the laboratory of K.K., were bred in-house to produce the experimental TS4Cre-BMAL1^{lox} mice used in this study (hereafter cBMAL1KO). At 21-days of age, genotyped male and female TS4Cre (control) and cBMAL1KO mice were weaned and group housed 2 to 5 mice per cage by genotype. At 5 to 7 weeks of age, mice were single housed into chambers specifically designed to conduct circadian experiments in rodents (ie, light-tight, well-ventilated chambers that allow for manipulation of light-dark cycles independent of the ambient room lighting conditions). Mice were maintained on a standard 12-hour light-dark (8 AM to 8 PM) schedule and were provided food ad libitum. Half of the male and female mice from each group received 2% DSS in the drinking water for 5 days, while the other mice received only water (**Supplementary Figure 1**). Mice were sacrificed on day 9, after 3 days of recovery from DSS.[10] Daily weight, stool consistency, and presence of hematochezia were documented each morning. The central circadian rhythm was assessed by wheel running activity and is detailed in the Supplementary Methods.

Crypt Isolation

Crypts were isolated from fresh colonic tissue and were used to assess BMAL1 protein levels in the colon IECs of the TS4Cre and cBMAL1KO mice using Western blot. Detailed methods are presented in the Supplementary Methods.

Hematoxylin and Eosin Staining

To assess histologic changes, sections (4- to 5-μm thickness) of fixed colon tissue samples were stained with hematoxylin and eosin, as previously described.[15] Samples were scored blindly by a gastrointestinal pathologist who assessed intestinal inflammation and tissue injury. Seven score categories were used to measure colon tissue destruction, inflammation, and repair, as described in the Supplementary Methods.

Intestinal Permeability

In vivo intestinal permeability was determined at the end of the experiment, as previously described.[16] The test was performed at zeitgeber time 0, after mice had been fasted overnight. A 200-µL solution containing lactulose (3.2 mg), sucrose (0.45 mg), sucralose (0.45 mg), and mannitol (0.9 mg) was administered via gavage, after which 2 mL of lactated ringers was administered subcutaneously to promote urine output. Mice were placed in metabolic cages for 5 hours, after which urine was collected and the total volume recorded. Intestinal permeability was calculated using gas chromatography to measure urinary sugar concentration. Permeability is expressed as percent excretion of oral dose of sugar.[17]

Immunofluorescence Staining

The colon tissue immunofluorescence (IF) staining was performed on slides. Specifics regarding IF staining are detailed in the Supplementary Methods. All tissue staining data are from 4 mice per group, with images from at least 10 stained tissue fields used to determine relative expression of each marker and to select representative images. All staining images were evaluated by 2 blinded, independent observers using a Zeiss LSM 700 confocal microscope (Zeiss, Oberkochen, Germany). All images were taken at ×20 magnification.

Western Blotting Analysis

Mouse colon tissue was lysed with Tris-triton buffer (Bioworld; Fisher, Pittsburgh, PA, USA) with a phosphatase/protease inhibitor cocktail (Sigma-Aldrich, St. Louis, MO, USA). For Western blots, total protein was determined (Bio-Rad, Hercules, CA, USA), and samples were prepared with Laemmli sample buffer with 2-ME (Bio-Rad). Twenty micrograms of protein/lane was loaded into a 4%/7.5% stacking acrylamide Tris gel and electrophoresed at 100 V for 2.5 hours. Protein was then transferred to a nitrocellulose membrane (GE Healthcare, Buckinghamshire, United Kingdom) overnight at 30 V. Nonspecific binding was blocked by incubation of the membrane with 5% bovine serum albumin/Tris-buffered saline with 0.1% Tween 20 detergent (TBST) for 1 hour. Membranes were then incubated overnight at 4°C with antibodies for zonula occludens-1 (ZO-1) (cat # 61-7300; Invitrogen, Waltham, MA, USA) or h-actin (cat #A4700; Sigma-Aldrich) in TBST. Membranes were subsequently washed with TBST for 1 hour and incubated with the appropriate horseradish peroxidase–conjugated anti-secondary antibody. Chemiluminescent substrate (ECL; GE Healthcare) was applied to the membrane for protein visualization using autoradiography film (HyBlot CL; Denville Scientific, Metuchen, NJ, USA). Optical density was determined via densitometric analysis with ImageJ version 1.42 software (National Institutes of Health, Bethesda, MD, USA). Data were normalized to actin for each lane for densitometry comparisons.

Serum Cytokines

Levels of interleukin (IL)-6 and tumor necrosis factor alpha (TNF-α) in serum were determined by enzyme-linked immunosorbent assay using Quantikine kits (R&D Systems, Minneapolis, MN, USA), according to the manufacturer's recommendations. Results were read by colorimetry on a BioTek Synergy multiwell plate reader (BioTek, Winooski, VT, USA) at wavelength 450 nm.

Gas Chromatography–Tandem Mass Spectrometry

The quantitation of the SCFA acetic acid, butyric acid, isovaleric acid, lactic acid, propionic acid, and succinic acid was performed using isotope dilution gas chromatography–tandem mass spectrometry by using MRM mode. The absolute quantity of each SCFA was determined using calibration curves measured for each analyte. Measurements were normalized to sample dry weight. This was achieved by separating the stool samples into 2 pieces of equal weight (wet weight): one piece was processed for derivatization and the other piece was dried overnight and then reweighed (dry weight). Dry weight normalization was calculated as (wet weight) × (dry weight/wet weight). Samples were analyzed by using the Thermo TSQ-Evo triple quadrupole in tandem with the Trace 1310 gas chromatograph (Thermo Fisher Scientific, Waltham, MA, USA). The remainder of these methods are described in the Supplementary Methods.

Sample Collection, DNA Extraction, and DNA Sequencing

Male mice stool pellets were collected and stored at -80°C until analysis. Total genomic DNA was extracted from the feces using the FastDNA SPIN Kit from the manufacturer's protocol (FastDNA Spin Kit for Soil; MP Biomedicals, Solon, OH, USA). DNA concentrations were measured with fluorometric quantitation (Qubit 3.0; Life Technologies, Grand Island, NY, USA). Primers 515F/806R (515F: GTGYCAGCMGCCGCGGTAA; 806R: GGACTACNVGGGTWTCTAAT), targeting variable region 4 (V4) of microbial small subunit (SSU or 16S) ribosomal RNA genes, were used and prepared for high-throughput amplicon sequencing using a 2-stage percutaneous coronary intervention method. Negative control animals were used with each set of amplifications, which indicated no background contamination. Sequencing was performed using an Illumina MiSeq (Illumina, San Diego, CA, USA), with a V2 kit and paired-end 250 base reads at the Genome Research Core at the University of Illinois at Chicago. Raw sequence data (FASTQ files) were deposited in the National Center for Biotechnology Information Sequence Read Archive under BioProject PRJNA627195.

16S Ribosomal RNA V4 Sequencing Analysis

Raw sequences obtained were merged using the PEAR (paired-end read merger) algorithm (v0.9.11; https://cme.h-its.org/exelixis/web/software/pear/). Merged sequences were then quality filtered using cutadapt and denoised using the DADA2 algorithm within the QIIME2 (v 2020.8.0; https://qiime2.org/) workflow. The produced amplicon sequence variants were used in all downstream analysis. Taxonomy was assigned to amplicon sequence variants by using the naïve Bayes taxonomy classifier against the SILVA 138 99% OTU database reference sequences. Please reference the Supplementary Methods for additional details.

Statistical Analysis

A 2-way repeated measures (RM) analysis of variance (ANOVA) was used to detect genotype and time effects in disease activity index (DAI) outcomes. A 4-way RM ANOVA

was used to determine genotype, time, treatment, and sex effects from percent change in body weight measurements. A 3-way ANOVA was used to detect a genotype, treatment, and sex effects of histology severity of colitis scores. A 2-way ANOVA was used to detect genotype and treatment effects in the male and female comparison of colon length, and for only the male mice comparisons of urine intestinal permeability, colonic epithelial apical junction proteins, serum cytokines, messenger RNA (mRNA), alpha diversity indices, fecal SCFA metabolomics measurements, and the percent relative abundance of SCFA-producing bacteria. All these analyses were corrected for multiple comparison testing using the Benjamini-Hochberg method with adjusted P values (q values). An independent t test was used to assess differences in histology scores. The chi-square test was used to assess differences in mortality. Significance levels were set at $P < .05$ in all analyses. Statistics were performed using GraphPad Prism (v9.0; GraphPad Software LLC, San Diego, CA, USA) and SPSS Statistics V26 (IBM, Armonk, NY, USA). Analyses of alpha and beta diversity were used to examine changes in fecal microbial community structure. Details of the microbiota statistical analysis are found in the Supplementary Methods.

Ethical Considerations

Rodent studies were approved by the Rush University Medical Center Institutional Animal Care and Use Committee. All methods were carried out in accordance with relevant guidelines and regulations.

Results

Murine Model

Central circadian rhythm assessment

In order for us to evaluate our animal model, we needed to first show that central circadian rhythms in our cBMAL1KO mice were intact. Rest-wake activity was monitored continuously in 5 cBMAL1KO mice and 5 TS4Cre control mice via wheel running over 2 weeks of standard 12-hour light-dark conditions followed by 2 weeks of dark-dark conditions to evaluate the endogenous circadian period. There was no significant difference in periods between the groups in either condition. Under dark-dark conditions (24 hours of dark), TS4Cre mice had a mean period of 23.7 ± 0.15 hours and cBMAL1KO mice had a mean period of 23.8 ± 0.67 hours (independent t test: $P = .11$) (**Supplementary Figure 2A and 2B**). Similarly, cBMAL1KO and TS4Cre mice exhibited normal actograms of their activity during the experimentation under 12-hour light-dark cycles (**Supplementary Figure 3**), showing no difference in activity or entrainment during the study.

BMAL1 protein levels in colon epithelium

To assess the efficiency of BMAL1 knockout in the colonic tissue, we isolated colonic epithelial crypts and analyzed protein levels of BMAL1 (**Supplementary Figure 2C**). Intestinal tissue contains many cell types including IECs, and isolation of crypts allows for more accurate assessment of BMAL1 in IECs due to a relative increase in IECs in the sample after removal of non–crypt cell types (eg, immune cells). cBMAL1KO mice had significantly lower levels of BMAL1 protein than TS4Cre mice (independent t test: $P = .015$) indicating that the knockout was successful. It is important to note that the isolated crypts contained different cell types (other than differentiated enterocytes) that do not express TS4, such as goblet cells, Tuft cells, and neuroendocrine cells; therefore, it was expected to have some remaining low BMAL1 levels in our crypt preparation from TS4Cre mice.

Severity of DSS-Induced Colitis

Disease activity index

The DAI incorporates daily body weight changes, stool consistency, and hematochezia. Higher scores indicate greater ulcerative colitis–like symptoms. After treatment with DSS, cBMAL1KO mice had significantly higher DAI than TS4Cre mice (**Figure 1A**). Analysis via a 2-way RM ANOVA for male mice revealed a significant time (ie, disease course) effect ($F_{9,155} = 270.6$, $P < .0001$), as cBMAL1KO + DSS had earlier symptoms than TS4Cre + DSS, as well as a genotype effect ($F_{1,155} = 462.9$, $P < .0001$) and interaction (time × genotype) effect ($F_{9,155} = 74.18$, $P < .0001$). Likewise, a 2-way RM ANOVA for female mice treated with DSS revealed a significant time effect ($F_{9,158} = 263.4$, $P < .0001$), genotype effect ($F_{1,158} = 235.3$, $P < .0001$), and interaction (time × genotype) effect ($F_{1,158} = 40.17$, $P < .0001$). Multiple comparison analysis revealed a genotype difference in colitis severity: cBMAL1KO + DSS male mice had significantly higher DAI on days 4 to 8 than TS4Cre + DSS mice ($q < 0.0001$), while cBMAL1KO + DSS female mice had significantly higher DAI on days 4-6 than TS4Cre + DSS ($q < 0.0001$). Taken together, these results suggest that DSS-induced colitis is worse in mice with a disrupted peripheral circadian rhythm. Interestingly, female cBMAL1KO mice appeared more resilient to DSS as compared with male cBMAL1KO mice, as their DAI showed earlier improvement.

Mortality

Mortality of DSS-treated mice was monitored and depicted (**Figure 1A**). Overall, 7 (28%) of 25 of male cBMAL1KO + DSS mice died, while none of the 16 male TS4Cre + DSS mice died (chi-square: $P = .025$). Similarly, more female cBMAL1KO + DSS mice died (n = 4 of 25, 16%) compared with female TS4Cre + DSS mice (n = 1 of 21, 4.8%), but this difference was not statistically significant (chi-square: $P = .22$). This indicates that disruption of colon circadian homeostasis significantly increased mortality in DSS-treated male mice.

Percent change in daily body weight

Daily body weight was recorded and depicted (**Figure 1B**). The cBMAL1KO mice developed significantly decreased body weight with DSS treatment as compared with TS4Cre control animals with and without DSS treatment. A 4-way RM ANOVA revealed significant differences for time (ie, disease course) effect ($F_{9,703} = 4.967$, $P < .001$), genotype effect ($F_{7,703} = 22.51$, $P < .0001$), and treatment effect ($F_{7,703} = 45.02$, $P < .0001$) but revealed no sex effect. There was a significant interaction between genotype and treatment ($F_{49,703} = 3.752$, $P < .001$) but no interactions between genotype and sex; treatment and sex; or genotype, sex, and treatment. Multiple comparison analysis indicated the following: TS4Cre + DSS male mice had significant weight loss compared with TS4Cre male control animals on days 6 to 9 ($P < .05$), cBMAL1KO + DSS male mice had significant weight loss compared with cBMAL1KO male control animals on days 3 to 9 ($P < .05$),

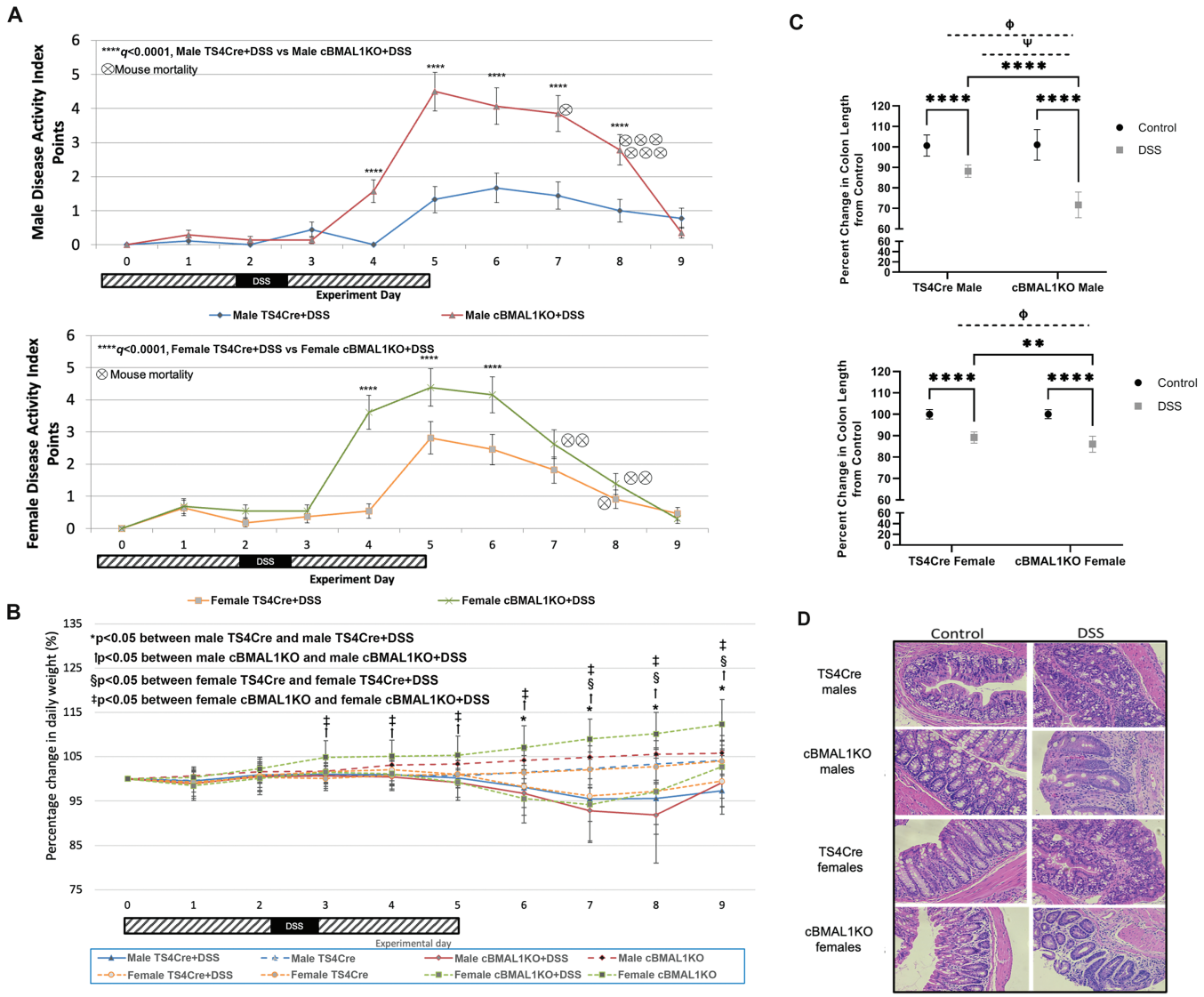

Figure 1. Dextran sulfate sodium (DSS) induces changes on the intestine that are sex and genotype dependent. These analyses were conducted in both female and male mice. A, Disease activity indices (DAIs) for male mice (top) and female mice (bottom). Multiple comparison analysis revealed that cBMAL1KO + DSS male mice had significantly higher DAI on days 4 to 8 than TS4Cre + DSS male mice, and cBMAL1KO + DSS female mice had significantly higher DAI on days 4 to 6 than TS4Cre + DSS female mice: ****$q < 0.0001$. Additionally, mortality is demonstrated on these graphs: ⊗. Mortality rate for cBMAL1KO + DSS male mice was 7 (28%) of 25, while no TS4Cre + DSS male mice died (chi-square: $P = .025$). The mortality rate for cBMAL1KO + DSS female mice was 4 (16%) of 25 and 1 (4.8%) of 21 for TS4Cre + DSS female mice (chi-square: $P = .22$). B, Percent change in weight by group. Multiple comparison analysis indicated TS4Cre + DSS male mice had significant weight loss compared with TS4Cre control male mice on days 6 to 9 ($P < .05$). cBMAL1KO + DSS male mice had significant weight loss compared with cBMAL1KO control male mice on days 3 to 9 ($P < .05$). TS4Cre + DSS female mice had significant weight loss compared with TS4Cre control female mice on days 7 to 9 ($P < .05$). cBMAL1KO + DSS female mice had significant weight loss compared with cBMAL1KO control female mice on days 3 to 9 ($P < .05$). C, Colon lengths for male mice (top) and female mice (bottom). Multiple comparison analysis indicated that both male and female TS4Cre and cBMAL1KO mice had significant DSS-induced colon shortening compared with their respective control animals ($q < 0.0001$). Both cBMAL1KO + DSS male mice and female mice had more colon shortening, as compared with TS4Cre + DSS male mice ($q < 0.0001$) and female mice ($q < 0.004$): **$q < 0.01$; ****$q < 0.0001$; ϕ$P < .05$ for treatment effect; Ψ$P < .05$ for genotype effect. Male and female TS4Cre DSS-induced mice did not differentiate between colon lengths (independent t test: $P = .456$), whereas male cBMAL1KO + DSS indicated a significant shorter colon length as compared with female cBMAL1KO + DSS (independent t test: $P < .0001$). D, Histology for TS4Cre and cBMAL1KO male mice and female mice with and without DSS. A 3-way analysis of variance revealed that there was a treatment effect ($P < .0001$) and genotype effect ($P < .0007$) but there was no difference in sex effect for histology scores.

TS4Cre + DSS female mice had significant weight loss compared with TS4Cre female control animals on days 7 to 9 ($P < .05$), and cBMAL1KO + DSS female mice had significant weight loss compared with cBMAL1KO female control animals on days 3 to 9 ($P < .05$). Collectively, this suggests that DSS-induced colitis leads to significant weight loss in mice in both genotypes.

Intestinal Inflammation

Colon length

Colon length was measured and scored as a percent change from control (ie, non-DSS mice) (Figure 1C). A 2-way ANOVA analysis on male mice revealed significant genotype effect ($F_{1,36} = 19.43$, $P < .001$), treatment effect ($F_{1,36} = 131.1$, $P < .001$), and interaction (genotype × treatment) effect

($F_{1,36}$ = 21.16, P < .001). Female mice only had a significant treatment effect ($F_{1,35}$ = 205.9, P < .001), with no differences for genotype effect or interaction (genotype × treatment) effect. Multiple comparison analysis indicated that both male and female TS4Cre and cBMAL1KO mice had significant DSS-induced colon shortening compared with their respective control animals (q < 0.0001), suggesting the presence of colonic inflammation with DSS. The cBMAL1KO + DSS male mice had more colon shortening, as compared with TS4Cre + DSS male mice (q < 0.0001), plus cBMAL1KO + DSS female mice had more colon shortening as compared with TS4Cre + DSS female mice (q = 0.004). Furthermore, the male and female TS4Cre DSS-induced mice did not differentiate between colon lengths (independent t test: P = .456). However, male and female cBMAL1KO mice treated with DSS indicated a significant difference between colon length (independent t test: P < .0001). Male cBMAL1KO + DSS mice had greater colon shortening compared with female cBMAL1KO + DSS mice. Overall, these data demonstrate that the male cBMAL1KO mice developed more significant colitis with DSS compared with male and female TS4Cre mice and female cBMAL1KO mice.

Histological severity of colitis (hematoxylin and eosin staining)

Colon tissue from mice that did not receive DSS did not exhibit any histological evidence of inflammation or tissue damage. The mice groups treated with DSS all demonstrated increased histologic scores in the injury model (**Figure 1D**, **Table 1**). A 3-way ANOVA analysis revealed that there was a treatment effect ($F_{1,71}$ = 22.55, P < .0001) and a genotype effect ($F_{1,71}$ = 12.66, P < .0007) but no sex effect. There was a significant interaction between treatment and genotype ($F_{1,71}$ = 11.68, P < .001).

Rationale for focusing on male mice for further analysis

Because our data showed significantly worse DSS-induced colitis phenotype (by DAI, mortality, and colon length) in male mice, male mice were chosen for further analysis of colonic barrier function, mucosal inflammation, and stool microbiota structure and function. Therefore, all subsequent analyses were performed on male TS4Cre and male cBMAL1KO mice.

Intestinal Permeability

Male in vivo measurement of intestinal permeability

Increased urinary sucralose and sucralose/lactulose ratio is a surrogate marker for increased colonic barrier permeability and colonic IEC barrier dysfunction.[17] Urinary sucralose excretion in male mice demonstrated a significant treatment effect (2-way ANOVA: $F_{1,34}$ = 32.58, P < .0001) but no genotype or interaction effects (**Figure 2A**). Multiple comparison analysis showed significantly increased (q < 0.0001) urinary sucralose excretion in both DSS-treated male mice groups compared with their respective control animals (**Figure 2A**). Furthermore, the urinary sucralose/lactulose ratio showed both a significant genotype effect (2-way ANOVA: $F_{1,34}$ = 9.247, P = .0045) and treatment effect (2-way ANOVA: $F_{1,34}$ = 23.95, P < .0001) (**Figure 2B**). Multiple comparison analysis showed significantly increased (q < 0.0001) sucralose-to-lactulose ratio in both DSS-treated male mice groups compared with their respective control animals, as well as a significantly enhanced sucralose-to-lactulose ratio in male cBMAL1KO + DSS mice (q = 0.0019) when compared with male TS4Cre + DSS mice (**Figure 2B**). These data indicate that DSS increases colonic barrier permeability and IEC barrier dysfunction and support our hypothesis that disruption of the circadian homeostasis in colon IEC increases vulnerability of the colon to the effects of DSS, resulting in worse DSS-induced disruption of the colonic barrier and inflammation.

Male ex vivo assessment of colonic epithelial apical junction proteins

AJC proteins (ZO-1, claudin-2, occludin, and E-cadherin) play a major role in intestinal epithelial barrier function. Therefore, we assessed AJC proteins in the colon of DSS-treated male cBMAL1KO mice and control animals using IF techniques. The ZO-1 protein expression was assessed by immunoblotting and showed significant differences with genotype (2-way ANOVA: $F_{1,25}$ = 10.82, P = .003) and treatment (2-way ANOVA: $F_{1,25}$ = 6.671, P = .016) (**Figure 2C**). When compared with TS4Cre control male mice, multiple comparison analyses showed significantly decreased ZO-1 protein expression in both TS4Cre + DSS (q < 0.015) and cBMAL1KO control (q < 0.001) mice. Claudin-2 is a pore-forming junction protein and an increase is consistent with barrier dysfunction. Claudin-2 protein expression demonstrated a treatment effect (2-way ANOVA: $F_{1,37}$ = 4.167, P = .048), indicating that its expression is increased after treatment with DSS, but no significant genotype or interaction effects (**Figure 2D**). Occludin protein expression was not different between mice groups (**Figure 2E**). E-cadherin demonstrated both a significant genotype effect (2-way ANOVA: $F_{1,48}$ = 4.323, P = .043), indicating decreased expression in circadian-disrupted mice, and treatment effect (2-way ANOVA: $F_{1,48}$ = 5.427, P = .024), indicating that DSS treatment decreases its expression in colon epithelium (**Figure 2F**). Altogether, the derangement of these AJC proteins is consistent with the intestinal barrier dysfunction

Table 1. Histology score comparisons in both male and female mice control and DSS groups

Mice Group	Control		DSS	
	Median	95% CI	Median	95% CI
TS4Cre male mice	0.00	0-0.55	2.50	0.84-4.16
cBMAL1KO male mice	0.00	0-1.11	4.50	3.75-16.1
TS4Cre female mice	0.00	0-0.45	0.00	0.03-2.97
cBMAL1KO female mice	0.00	0-0.45	12.00	6.77-17

Abbreviations: CI, confidence interval; DSS, dextran sulfate sodium.

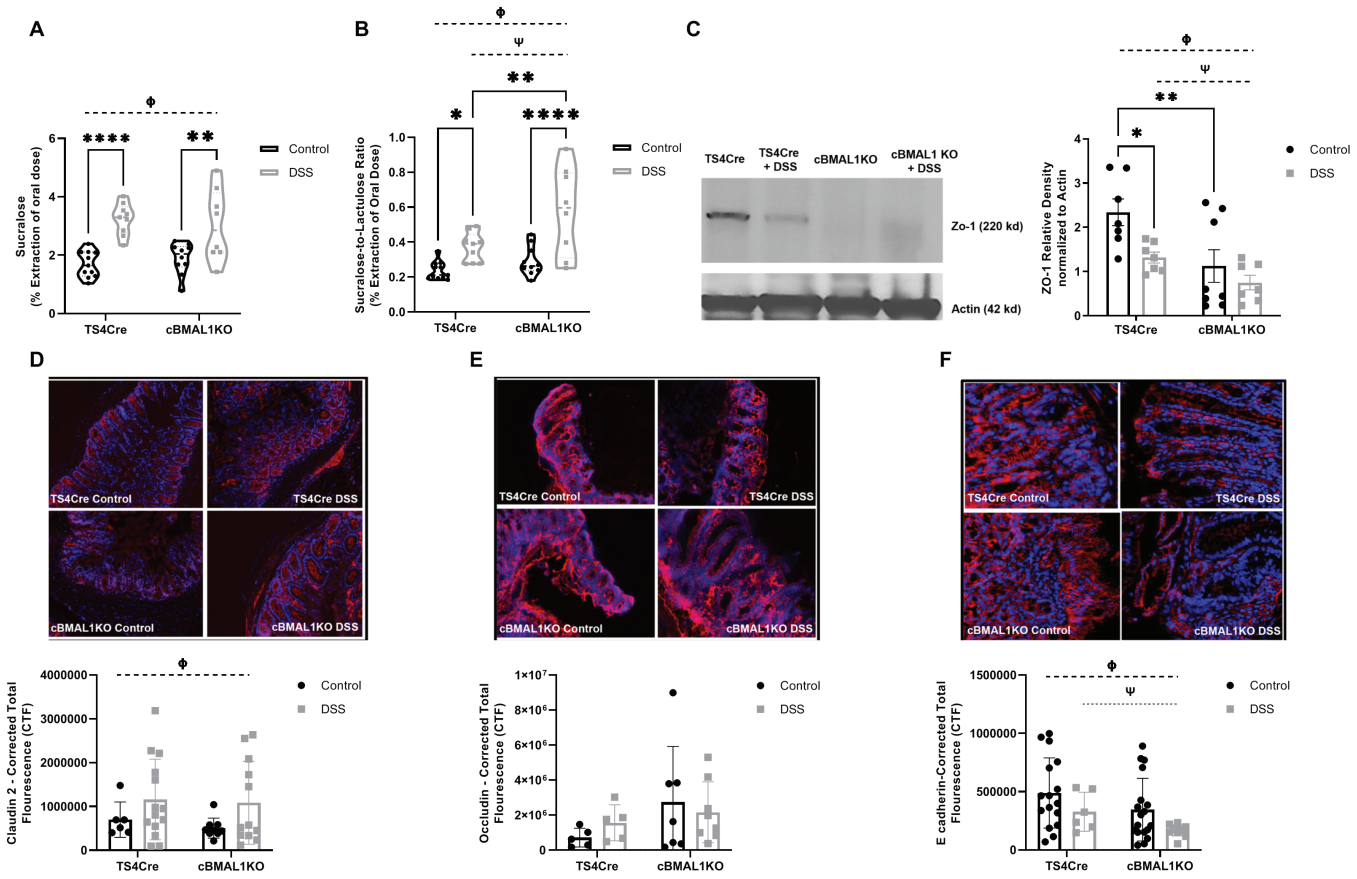

Figure 2. Dextran sulfate sodium (DSS) induces changes on the intestinal barrier that are genotype dependent. These analyses were conducted only in male mice. A, In vivo permeability demonstrated by percent excretion of oral dose of sucralose. A significant treatment effect was observed ($P < .0001$). Multiple comparison analysis showed significantly increased sucralose permeability in both DSS-treated male mice groups compared with their respective control animals. B, In vivo permeability demonstrated by the ratio or percent excretion of oral dose of sucralose to lactulose. A significant treatment effect ($P < .0001$) and genotype effect ($P = .0045$) were found. Multiple comparison analysis showed significantly increased sucralose-to-lactulose ratio permeability in both DSS-treated male mice groups compared with their respective control animals, as well as that the cBMAL1KO + DSS male mice sucralose-to-lactulose ratio significantly enhanced when compared with TS4Cre + DSS male mice. C, Immunoblotting for ZO-1 revealed a significant effect of genotype ($P = .003$) and treatment ($P = .016$). D, Immunofluorescence staining for claudin-2 revealed a significant treatment effect ($P = .048$) but no genotype effect. E, Immunofluorescence staining for occludin demonstrated no effects of treatment or genotype. F, Immunofluorescence staining for E-cadherin revealed a significant effect of genotype ($P = .043$) and treatment ($P = .024$). Statistical analyses included 2-way analysis of variance corrected for multiple testing using the Benjamini-Hochberg method. *$q < 0.05$; **$q < 0.01$; ****$q < 0.0001$; ϕ$P < .05$ for treatment effect; Ψ$P < .05$ for genotype effect.

supported by the in vivo permeability data. Collectively, these data suggest that peripheral circadian rhythm disruption disrupts IEC barrier function through decreased E-cadherin expression, which is further exacerbated by DSS administration. In addition, exposure to DSS increased pore-formation and gut leakiness through increased levels of claudin-2.

Inflammation

Male serum cytokines

One important consequence of intestinal barrier dysfunction is intestinal inflammation (as indicated by colon shortening), as well as systemic inflammation. We examined levels of various cytokines in the serum. Serum IL-6 was not significantly different between genotypes or treatment groups by 2-way ANOVA analysis. However, multiple comparison analysis revealed a significant difference between male cBMAL1KO + DSS and male cBMAL1KO control animals ($P = .016$) (**Figure 3A**). Serum TNF-α exhibited only a treatment effect (2-way ANOVA: $F_{1,25} = 10.34$, $P = .004$) (**Figure 3B**). Multiple comparison analysis showed that the serum TNF-α level was significantly elevated ($q < 0.02$) in male TS4Cre + DSS mice compared with TS4Cre mice.

Male mRNA expressions and STAT3 assessment in DSS model of colitis

Claudin-2 mRNA expression demonstrated a treatment effect (2-way ANOVA: $F_{1,15} = 5.648$, $P = .0312$) in male mice (**Supplementary Figure 4A**). Multiple comparison analysis indicated that male cBMAL1KO + DSS mice had significantly higher claudin-2 expression than male cBMAL1KO mice ($P = .010$). Occludin expression had a genotype effect (2-way ANOVA: : $F_{1,16} = 5.144$, $P = .0375$) in male mice (**Supplementary Figure 4B**). Occludin expression was significantly reduced in male cBMAL1KO mice compared with male TS4Cre mice ($P = .013$). When E-cadherin expression was explored, it showed no differences for treatment or genotype effects in male mice (**Supplementary Figure 4C**).

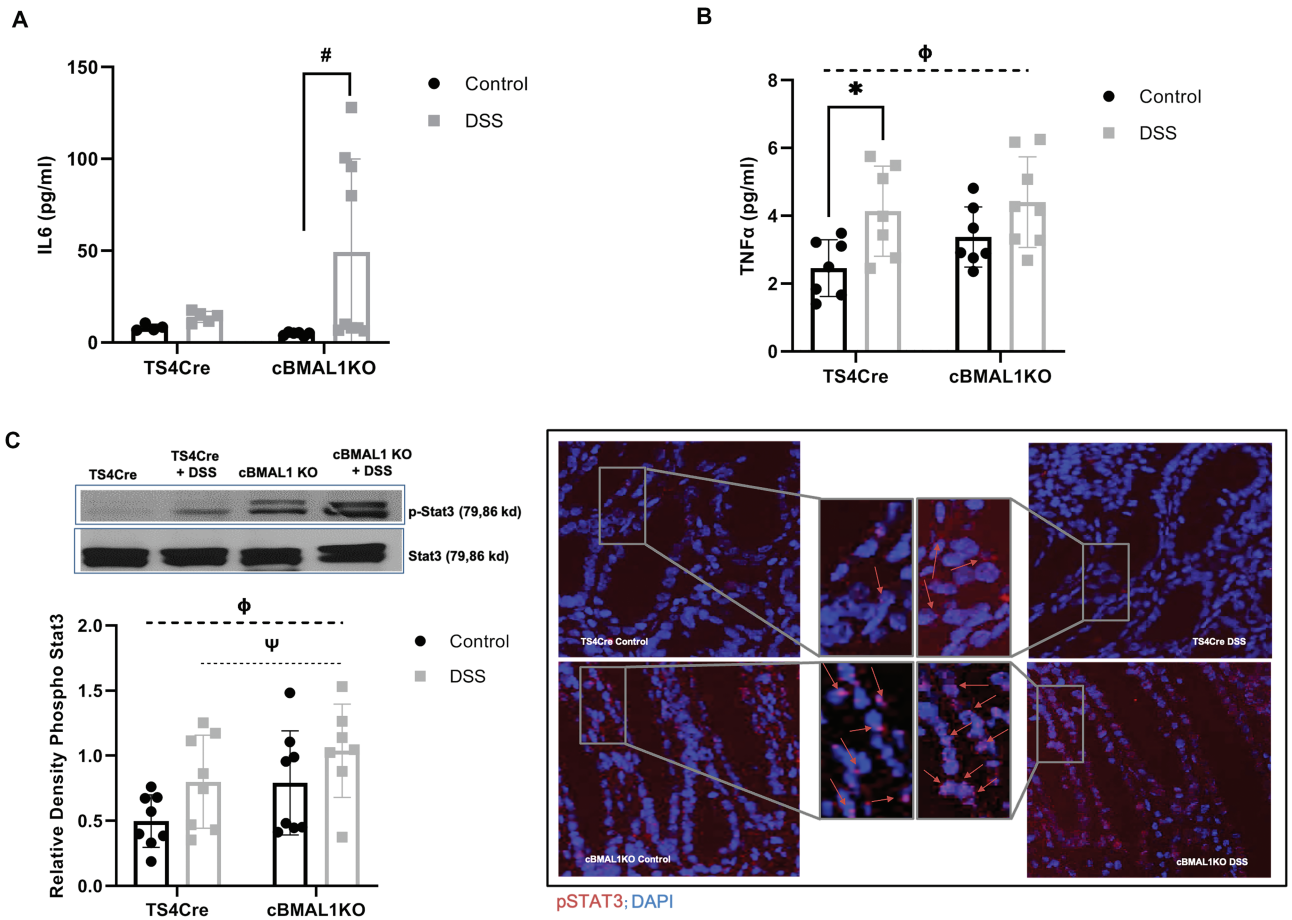

Figure 3. Systemic and intestinal inflammation are genotype dependent. These analyses were conducted only in male mice. A, Serum interleukin (IL)-6 did not indicate a significant difference for genotype or treatment effects. However, multiple comparison analysis was significantly different between cBMAL1KO control and cBMAL1KO + DSS male mice (P = .016) B, Serum tumor necrosis factor alpha (TNF-α) exhibited only a treatment effect (P = .004). Multiple comparison analysis showed that the serum TNF-α level was significantly elevated (q < 0.02) in the TS4Cre + DSS compared with TS4Cre control male mice. C, Western blot analysis of phospho-STAT3 (pSTAT3) protein exhibited both a treatment effect (P = .032) and genotype effect (P = .038) Immunohistochemistry stains of pSTAT3 and DAPI in the colons of the mice with and without DSS. Statistical analyses included 2-way analysis of variance corrected for multiple testing using the Benjamini-Hochberg method. #P < .05; *q < 0.05; ϕP < .05 for treatment effect; ΨP < .05 for genotype effect.

STAT3 mRNA expression demonstrated a treatment effect (2-way ANOVA: : $F_{1,16}$ = 6.275, P = .023) in male mice, with higher levels found in DSS-treated mice (Supplementary Figure 4D). Furthermore, Western blot analysis of phospho-STAT3 (pSTAT3) protein exhibited both a treatment effect (2-way ANOVA: $F_{1,27}$ = 5.108, P = .032) and a genotype effect (2-way ANOVA: $F_{1,27}$ = 4.755, P = .038), showing increased levels in mice treated with DSS as well as in mice with disrupted peripheral circadian rhythms (Figure 3C). IF staining density of pSTAT3 was significantly higher in colon tissue of male cBMAL1KO + DSS as compared with TS4Cre + DSS (Figure 3C), suggesting a possible key role of STAT3 in worsening of DSS-induced colitis with disruption of circadian homeostasis in the intestinal epithelial cells.

Microbiome

Male microbiome sequencing

As previously mentioned, this analysis was only assessed in male mice, as they exhibited a more severe colitis phenotype than female mice. Fecal samples were sequenced and data were compared as followed: (1) TS4Cre and cBMAL1KO male mice, (2) TS4Cre + DSS and cBMAL1KO + DSS male mice, (3) TS4Cre and TS4Cre + DSS male mice, and (4) cBMAL1KO and cBMAL1KO + DSS male mice. A total of 3 979 928 sequencing clusters were generated, with an average depth of 51 024 sequences per sample (median = 48 030 [range, 23 569-148 073]). The microbial communities were significantly different between the 4 male mice groups (principal coordinate analysis [PCoA]: Figure 4A; permutational multivariate ANOVA [PERMANOVA]: Table 2). Detailed genotypes and DSS-treated fecal microbiota comparisons results are depicted in the Supplementary Results.

Male murine model genotype microbiota

Microbial alpha diversity was measured for each sample to determine if there were differences in microbial community structure between TS4Cre and cBMAL1KO (Supplementary Table 1; Supplementary Figure 5). No significant differences in alpha diversity were observed for analyses conducted at the feature level. Beta diversity analyses revealed significant differences (false discovery rate P < .05) in fecal microbial community structure between TS4Cre and cBMAL1KO samples at the feature level (PCoA: Figure 4B; PERMANOVA: Table 2). Microbial communities were different and dominated

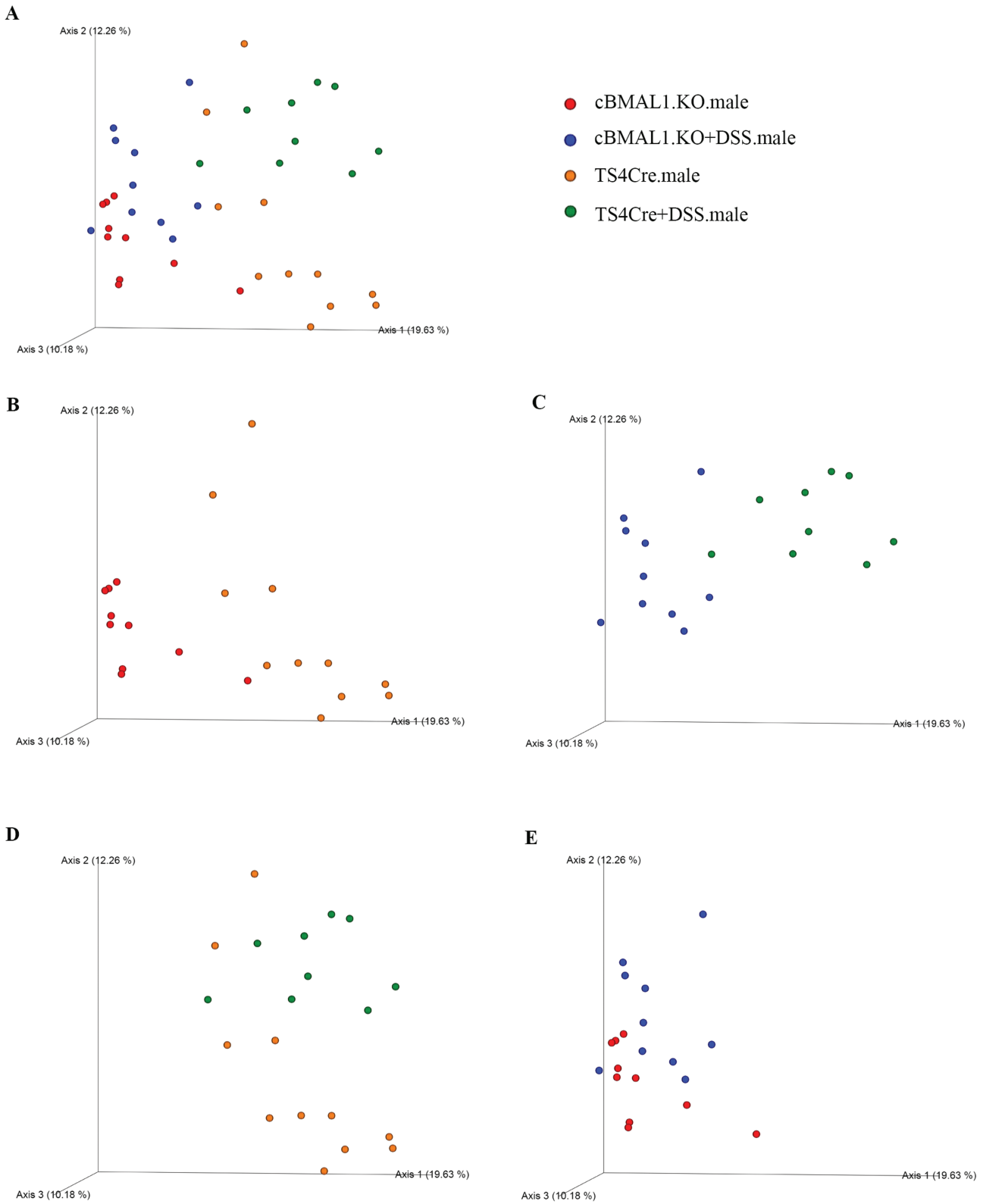

Figure 4. Principal coordinate analysis with Bray-Curtis dissimilarity. Results revealed that fecal samples clustered separately indicating that the fecal community is significantly different from each male mice group. Orientations of: A, 4 male mice sample groups; B, TS4Cre and cBMAL1KO samples; C, TS4Cre + DSS and cBMAL1KO + DSS; D, TS4Cre and TS4Cre + DSS; and E, cBMAL1KO and cBMAL1KO + DSS.

by bacteria from the phyla Bacteroidota and Firmicutes, and bacteria from the genera *Muribaculaceae*, *Bacteroides*, *Lachnospiraceae* spp., *Lactobacillus*, and *Helicobacter* (>50% of all sequences) (**Figure 5A and B**; **Supplementary Table 2**). Analysis revealed that compared with control mice, Firmicutes and other SCFA-producing microbiota were decreased in cBMAL1KO mice. Additional microbial taxa differing in abundance between TS4Cre and cBMAL1KO were identified

Table 2. Fecal microbial community structure differences between male mice group comparisons as assessed by PERMANOVA

Male Mice Comparison	Feature Taxonomic Level				
	Sample Size	Permutations	Pseudo-*F*	*P* Value	*q* Value
TS4Cre vs cBMAL1KO	21	9999	4.96	.0001[a]	0.0001[a]
TS4Cre + DSS vs cBMAL1KO + DSS	19	9999	4.82	.0001[a]	0.0001[a]
TS4Cre vs TS4Cre + DSS	20	9999	3.66	.0001[a]	0.0001[a]
cBMAL1KO vs cBMAL1KO + DSS	20	9999	1.93	.0245[a]	0.0245[a]

PERMANOVA results are based on Bray-Curtis distances for the multiamplicon (V4) sequence data at the feature level. Significant values are based on 9999 permutations and corrected for multiple testing using the Benjamini-Hochberg method ($q < 0.05$).
Abbreviations: DSS, dextran sodium sulfate; PERMANOVA, permutational multivariate analysis of variance.
[a]Threshold of significant difference for *P* and *q*-values < 0.05.

using DESeq2 and ANCOM (**Supplementary Tables 3 and 4**; **Supplementary Figure 6**). DESeq2 analysis indicated a total of 3 phyla and 32 genera, including a significantly ($q<0.05$) higher abundance of *Faecalibaculum* and significantly ($q<0.05$) lower abundances of *Lachnoclostridium*, *Mucispirillum*, *Candidatus Arthromitus*, and *Erysipelatoclostridium*, that are differentially abundant between control mice. ANCOM analyses identified 1 phylum (Deferribacterota; higher in TS4Cre) and 3 genera (all higher in cBMAL1KO) to be differentially abundant taxa that included *Faecalibaculum* (W score = 29), *Ruminococcaceae* uncultured (W score = 25), and *Alloprevotella* (W score = 24) (**Supplementary Tables 3 and 4**; **Supplementary Figure 6**). Furthermore, the percent relative abundance of putative SCFA bacterial genera demonstrated a genotype effect (2-way ANOVA: $F_{1,36} = 10.99$, $P = .0021$) in male mice. Multiple comparisons analyses for both the percent relative abundance of putative total SCFA bacteria genera ($q = 0.011$) and putative total butyrate bacteria genera ($P = .020$) were significantly lower in cBMAL1KO compared with TS4Cre male mice (**Figure 5C and D**). Taken together, this suggests that peripheral circadian rhythm disruption alters the gut microbiome, resulting in lower relative abundance of SCFA-producing bacteria, most notably a lower relative abundance of butyrate-producing bacteria.

Male murine model genotype and DSS microbiota

Microbial alpha diversity indices were compared between TS4Cre + DSS and cBMAL1KO + DSS mice. Indices were not significantly different between groups at the feature level (**Supplementary Table 1**; **Supplementary Figure 5**). However, fecal microbial community beta diversity differed between TS4Cre + DSS and cBMAL1KO + DSS mice (PCoA: **Figure 4C**; PERMANOVA: **Table 2**). Microbial communities were different and dominated by bacteria from the phyla Bacteroidota and Firmicutes, and bacteria from the genera *Muribaculaceae*, *Bacteroides*, *Lachnospiraceae* spp., *Lactobacillus*k, and *Helicobacter* (>50% of all sequences) (**Figure 5A and B**; **Supplementary Table 2**). Taxon-by-taxon analyses also identified significantly differently abundant genera between groups (**Supplementary Tables 5 and 6**). Overall, 2 phyla, Actinobacteria and Bacteroidota (both higher cBMAL1KO + DSS), and 24 genera were significantly differentially abundant between TS4Cre + DSS and cBMAL1KO + DSS mice. The cBMAL1KO + DSS mice had significantly higher abundance of genera *Faecalibaculum*, *Paraprevotella*, *Alloprevotella*, *Alistipes*, and *Murbaculaceae* and lower abundances of putative beneficial SCFA-producing bacteria *Lachnospiraceae* spp. (ASF356, UCG-001, FCS020), and *Staphylococcus* compared with TS4Cre + DSS (DESeq2: **Supplementary Table 6**). ANCOM identified 2 phyla, Bacteroidota (higher in cBMAL1KO + DSS) and Proteobacteria (higher TS4Cre + DSS), and 3 genera, *Candidatus Arthromitus* (W score = 30; higher TS4Cre + DSS) and *Faecalibaculum* (W score = 29) and *Paraprevotella* (W score = 25) (both higher in cBMAL1KO + DSS), to be significantly abundant between mice groups (**Supplementary Tables 5 and 6**). Furthermore, the percent relative abundance of putative proinflammatory bacteria-to-total SCFA ratio genera demonstrated a genotype effect (2-way ANOVA: $F_{1,35} = 6.644$, $P = .0143$) in male mice. Multiple comparisons analysis for the percent relative abundance of putative proinflammatory bacteria-to-total SCFA ratio genera was significantly higher ($P = .047$) in cBMAL1KO + DSS, compared with TS4Cre + DSS mice (**Figure 5E**). The putative proinflammatory genera examined in these comparisons included *Helicobacter*, *Alistipes*, *Rikenellaceae* RC9 gut group, *Parasutterella*, *Desulfovibrio*, *Odoribacter*, *Chlamydia*, Rhodospirillale Uncultured, *Rikenellaceae*, *Rikenella*, *Rodentibacter*, and *Escherichia-Shigella* (ie, closely related to *Escherichia coli*).[18] Overall, this shows that circadian rhythm disruption leads to a relatively higher relative abundance of putative proinflammatory bacteria after exposure to DSS.

Fecal SCFA metabolomics

Intestinal bacteria produce many metabolites, but one group that is particularly important for intestinal barrier integrity and inflammation is SCFAs. Accordingly, fecal SCFAs (acetate, propionate, and butyrate) and branched SCFAs (isovaleric acid, lactic acid, and succinic acid) were examined (**Supplementary Figure 7A-H**). Butyrate concentrations demonstrated a treatment effect (2-way ANOVA: $F_{1,36} = 4.727$, $P = .036$) in male mice. A multiple comparison test showed that butyrate concentrations were significantly lower in male TS4Cre + DSS ($q = 0.031$) and male cBMAL1KO ($q = 0.040$) mice as compared with male TS4Cre mice (**Supplementary Figure 7C**). Additionally, there was a significant treatment effect on butyrate-to-total SCFA ratio concentration (2-way ANOVA: $F_{1,36} = 6.029$, $P = .019$) in male mice. The butyrate-to-total SCFA ratio was significantly lower in TS4Cre + DSS ($q = 0.023$) compared with TS4Cre mice (**Supplementary Figure 7G**). Collectively, this could suggest that colon-specific circadian rhythm disruption creates a proinflammatory bacterial metabolite microenvironment in the colon, similar to the effects of DSS on control mice.

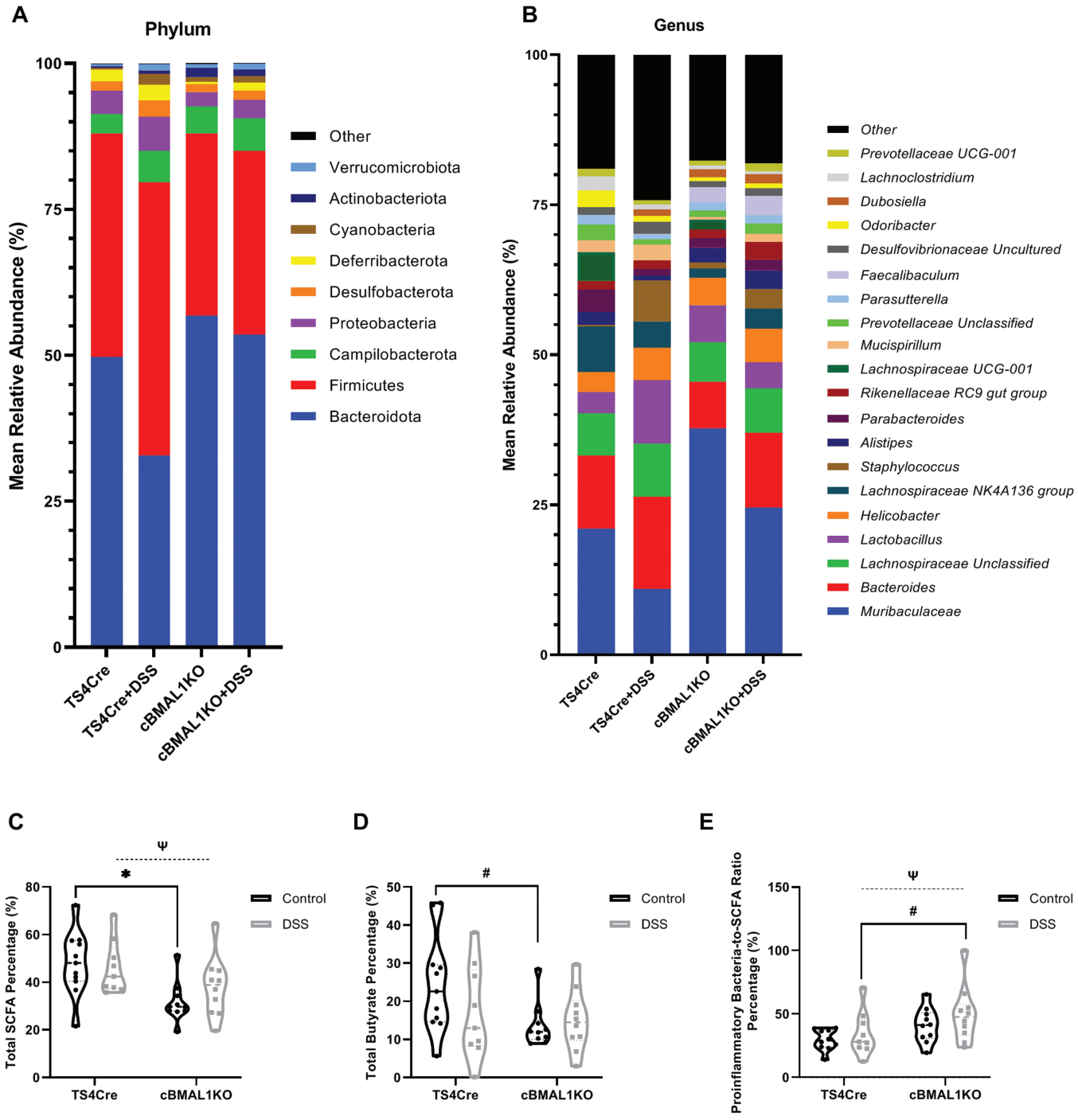

Figure 5. Microbial profiles of male TS4Cre and cBMAL1KO mice with and without dextran sulfate sodium (DSS). These analyses were conducted only in male mice. A, Stacked column plots depicting the percent mean relative abundance (>1%) of bacterial phyla. B, Stacked column plots depicting the percent mean relative abundance (>1%) of bacterial genera. Percent mean relative abundance of (C) total short chain fatty acid–producing taxa, (D) total butyrate-producing taxa, and (E) putative proinflammatory bacteria-to-total SCFA ratio examined are shown across mice groups. Statistical analyses included 2-way analysis of variance corrected for multiple testing using the Benjamini-Hochberg method. $^{\#}P < .05$; $^{*}q < 0.05$; Ψ $P < .05$ for genotype effect.

Discussion

The current study shows that peripheral circadian rhythm disruption in IEC (while central circadian rhythms remained intact) promoted (1) a profound increase in colitis severity and mortality in response to DSS administration, (2) alterations in the intestinal barrier with increased in vivo intestinal permeability, (3) increased intestinal inflammation including the proinflammatory mediator STAT3, and (4) changes in the fecal microbiota and SCFA metabolomics, with lower relative abundances of SCFA-producing bacteria and decreased fecal butyrate concentrations. Altogether, these findings identify disruption of the colon IEC circadian clock as a risk factor for more severe colitis.

Circadian rhythms are fundamental to health and normal physiology. Disruption of the central circadian rhythm through shift work or social jetlag is a common and important environmental factor promoting inflammatory disorders and metabolic syndrome.[19] Previous studies have shown that central circadian rhythm disruption can result in more severe colitis in rodent models, and markers of circadian misalignment are associated with more IBD complications in humans[10,11,20] as well as with decreased resiliency of the colon to injurious agents.[21,22] Alternatively, irregular and wrong-time eating, which is extremely common in modern society, is an example of peripheral circadian rhythm disruption in the gastrointestinal tract that has also been implicated in various diseases, including cancer and metabolic syndrome. Peripheral circadian rhythm disruption models isolate the effects of circadian rhythm disruption in a single organ (system) or cell type in order to minimize or avoid the impact of other organ systems, which is a common confounder in models of central circadian disruption. Intestinal IEC RORα-deficient mice showed increased inflammation in a DSS model,[23] and RORα is a key secondary feedback loop of the circadian clock. This study is the first to examine the effects of genetic disruption of core circadian machinery (BMAL1) in colonic epithelial cells on colonic barrier function, gut microbiota, and colitis severity in mice.

In establishing a clinical phenotype for these animals, we found a unique sex difference in colitis severity: the female cBMAL1KO mice demonstrated a less severe colitis phenotype than male cBMAL1KO mice after DSS treatment. While the male cBMAL1KO mice had more severe colitis demonstrated by prolonged disease course (high DAI), mortality rate, and reduced colon length compared with male TS4Cre mice, the female cBMAL1KO mice had a shorter disease course, and there was no difference in mortality or colon length, as compared with female TS4Cre mice. This is in keeping with other studies, which have demonstrated sex differences in DSS-induced colitis with female mice demonstrating more resistance to DSS.[24] In sex-specific immune responses, several studies demonstrated the importance of estrogen in T lymphocytes and in innate and adaptive immunity.[25] Central circadian disruption in humans also has sex-specific influences on energy homeostasis and metabolism[26] and cognition.[27] Future studies are needed to further investigate the mechanism involved in the sex differences demonstrated in this cBMAL1KO colitis model.

Based on our data, DSS-induced intestinal barrier dysfunction was mediated through an increase of pore forming claudin-2 and a decrease of adherence junction protein E-cadherin and ZO-1, which are all components of the AJC in the colonic epithelium responsible for maintaining normal intestinal barrier function. Indeed, claudin-2 is a pore-forming tight junction protein and increased levels lower transepithelial resistance and result in a more porous barrier,[28] while ZO-1 is a tight junction scaffolding protein that downregulation of may not alter the intestinal barrier at baseline, but rather results in defective intestinal barrier after injury.[29] This is not surprising, as tight junction protein expression in the intestine has been reported to be under circadian regulation.[30] The combination of increased pore formation (claudin-2) and decreased barrier-strengthening ZO-1 and apical junctions (E-cadherin) in response to DSS contributed to intestinal barrier dysfunction and worse DAI. Our data suggest that peripheral circadian rhythm disruption exacerbates these adverse changes in intestinal barrier function.

The STAT3 pathway is a well-established regulator of intestinal inflammation: STAT3-mediated activation of the adaptive immune system worsens colitis by enhancing the survival of pathogenic T cells, while STAT3-mediated activation of the innate immune system suppresses colitis.[31] Phosphorylation of STAT3 promotes translocation into the nucleus and changes in gene transcription that impact cellular function, immunity, and inflammation. pSTAT3 was elevated in actively inflamed colon tissue of patients with ulcerative colitis[32] and was correlated with the degree of inflammation seen on histology. In our study, genetic disruption of the peripheral circadian clock through knockout of BMAL1 in IECs significantly increased pSTAT3, even before chemical induction of colitis. This is in accordance with a prior study showing increased colonic pSTAT3 levels in mice with environmental disruption of intestinal circadian rhythm (induced by wrong-time feeding) and concurrent alcohol consumption, which was associated with colonic polyp formation through induction of protumorigenic inflammation.[8] Increased serum IL-6 and TNF-α are associated with increased phosphorylation of STAT3,[33] and previous in vitro studies found that STAT3 may play a critical role in upregulation of claudin-2[34] and downregulation of E-cadherin,[35] which is consistent with our findings. Thus, the mechanism by which peripheral circadian rhythm disruption promotes colitis and barrier dysfunction may be through pSTAT3-induced activation of T lymphocytes and upregulation of claudin-2 plus downregulation of E-cadherin, respectively. However, in order to confirm STAT3 as the mechanism of decreased resiliency to DSS-induced colitis in this model, loss- and gain-of-function of experiments of STAT3 would need to be performed in the future.

One additional key finding in the present study was that there were alterations in the microbial community structure in cBMAL1KO mice compared with control mice, even prior to DSS treatment, particularly with an increase in the genus *Faecalibaculum*, which has been associated with an increase susceptibility to DSS colitis (see Supplementary Figure 5).[36] Prior studies[37] have highlighted that circadian disruption in the host causes microbial alterations with decreased relative abundances in SCFA-producing bacteria, specifically derived from the phylum Firmicutes. These microbial changes are similar to findings in IBD patients' microbial profiles in which there is a decrease in bacterial diversity[38] and temporal stability,[39] with lower relative abundance of SCFA-producing bacteria associated to the phylum Firmicutes[40] and increased relative abundance of putative proinflammatory bacteria derived from the phylum Proteobacteria.[41] Analysis of fecal samples in this study revealed that there is a significant decrease in the relative abundance of SCFA-producing bacteria, along with a significant decrease in fecal butyrate metabolite concentrations in cBMAL1KO mice. The SCFA butyrate has several important biological effects: it induces epithelial cell proliferation, increases mucin production, is anti-inflammatory (lowers STAT3 levels), and provides protective effects on the epithelial barrier including facilitating AJC assembly and decreasing bacterial translocation.[42] In addition, cBMAL1KO mice had increased relative abundance of putative pro-inflammatory bacteria, indicating a pro-inflammatory intestinal microenvironment. The most well-known pathobiont, adherent-invasive species *E. coli*, has been linked with intestinal inflammation and barrier dysfunction in IBD,[43,44] and transcytosis of bacteria can often precede tight junction protein damage in IBD models.[45-47] These fecal microbial profiles support our findings that disruption of circadian rhythms

in IEC promotes subclinical inflammation that predisposes cBMAL1KO mice to more severe DSS-induced colitis.

There are several important limitations to this study. First, there are several important model limitations. We used the DSS model of colitis, which is mainly an epithelial damage model that does not exactly replicate human colitis. Future studies should examine other colitis models such as an IL-10 knockout that would incorporate changes in mucosal immune function. In addition, an environmental model studying the impact of wrong-time feeding to induce colonic circadian rhythm disruption in rodents would add to our findings in a genetic peripheral circadian rhythm disruption model. This study therefore provides a proof-of-concept for studying the effects of food timing on human subjects with IBD. Second, the exact mechanisms behind the phenotypic findings in the rodent model cannot be confirmed without further in vivo and in vitro analyses, such as loss and gain of function of STAT3, stool transplant to correct dysbiosis, or supplementation with SCFAs like butyrate. Third, further studies will be needed to understand the generalizability of this study in other models of peripheral circadian rhythm disruption.

In summary, this study demonstrates the significant impact of peripheral genetic circadian rhythm disruption of the colon epithelium in a rodent colitis disease model. We found that mice with disrupted circadian rhythms in colonic IEC had worse intestinal barrier dysfunction and more severe colitis after DSS treatment, suggesting that circadian rhythm disruption impairs resiliency of the colonic epithelium. This appeared to be mediated through changes in the intestinal microbiota favoring the relative abundances of putative proinflammatory bacteria and reducing the relative abundances of SCFA-producing bacteria, leading to decreased butyrate metabolite production and increased pSTAT3 levels, as well as to increased intestinal barrier permeability secondary to increased claudin-2 and decreased E-cadherin expression. Future studies should elucidate the exact molecular mechanism by which disrupted circadian rhythm in the colon epithelium worsens colonic injury and further investigate the potential role of the STAT3 signaling pathway through loss and gain of function, intestinal microbiota, and metabolites such as microbiota-derived SCFAs. These mechanistic studies could identify novel therapeutic target(s) to treat IBD.

Supplementary Data

Supplementary data is available at *Inflammatory Bowel Diseases* online.

Author Contribution

Conceived and designed the experiments: S.B.J., M.S., D.M.H, R.M.V., C.B.F., A.K., and G.R.S. Performed the experiments: S.B.J., M.S., P.A.E., S.W., M.J.B., and F.K. Analyzed the data: S.B.J., M.S., P.A.E., A.N., L.T., V.R., S.J.G., M.J.B., S.W., S.R, L.Z, S.S., G.S., V.C., and Z.P. Contributed materials: K.K. Wrote the manuscript: S.B.J., M.S., P.A.E., Z.P., M.J.B., R.M.V., C.B.F., A.K., G.R.S. Reviewed the manuscript: all authors.

Funding

This work was supported by a Pfizer Pharmaceuticals Inflammatory Bowel Disease Competitive Grant 2019 and a Pfizer Global Medical Grants Inflammatory Bowel Disease 2019 (grant 52438947), and additional funding was generously provided by philanthropy support of the Sklar family as well as Charles and Joanne Johnson. Additional support was provided by the National Institute on Alcohol Abuse and Alcoholism of the National Institutes of Health in part by grant R24AA026801 (to A.K.).The views expressed in the submitted articles the authors' own and are not the official position of the institution or funder.

Conflicts of Interest

The authors declare no competing interests.

Data Availability

All data are presented in this study. The authors will make materials, data, and associated protocols promptly available to readers without undue qualifications in material transfer agreements. There are no restrictions on the availability of the materials and information.

References

1. Lakatos PL, Kiss LS. Is the disease course predictable in inflammatory bowel diseases? *World J Gastroenterol.* 2010;16(21):2591-2599.
2. Swanson GR, Burgess HJ, Keshavarzian A. Sleep disturbances and inflammatory bowel disease: a potential trigger for disease flare? *Expert Rev Clin Immunol 2011*;7(1):29-36.
3. Scheiermann C, Kunisaki Y, Frenette PS. Circadian control of the immune system. *Nat Rev Immunol.* 2013;13(3):190-198.
4. Ruben MD, Wu G, Smith DF, et al. A database of tissue-specific rhythmically expressed human genes has potential applications in circadian medicine. *Sci Transl Med.* 2018;10(458):eaat8806.
5. Codoner-Franch P, Gombert M. Circadian rhythms in the pathogenesis of gastrointestinal diseases. *World J Gastroenterol.* 2018;24(38):4297-4303.
6. Yasumoto Y, Hashimoto C, Nakao R, et al. Short-term feeding at the wrong time is sufficient to desynchronize peripheral clocks and induce obesity with hyperphagia, physical inactivity and metabolic disorders in mice. *Metab Clin Exp.* 2016;65(5):714-727.
7. Almoosawi S, Prynne CJ, Hardy R, Stephen AM. Time-of-day and nutrient composition of eating occasions: prospective association with the metabolic syndrome in the 1946 British birth cohort. *Int J Obes (Lond).* 2013;37(5):725-731.
8. Bishehsari F, Engen PA, Voigt RM, et al. Abnormal eating patterns cause circadian disruption and promote alcohol-associated colon carcinogenesis. *Cell Mol Gastroenterol Hepatol.* 2020;9(2):219-237.
9. Amara J, Saliba Y, Hajal J, et al. Circadian rhythm disruption aggravates DSS-induced colitis in mice with fecal calprotectin as a marker of colitis severity. *Dig Dis Sci.* 2019;64(11):3122-3133.
10. Preuss F, Tang Y, Laposky AD, Arble D, Keshavarzian A, Turek FW. Adverse effects of chronic circadian desynchronization in animals in a "challenging" environment. *Am J Physiol Regul Integr Comp Physiol.* 2008;295(6):R2034-R2040.
11. Wang S, Lin Y, Yuan X, Li F, Guo L, Wu B. REV-ERBalpha integrates colon clock with experimental colitis through regulation of NF-kappaB/NLRP3 axis. *Nat Commun.* 2018;9(1):4246.
12. Moravcova S, Pacesova D, Melkes B, et al. The day/night difference in the circadian clock's response to acute lipopolysaccharide and the rhythmic Stat3 expression in the rat suprachiasmatic nucleus. *PLoS One.* 2018;13(9):e0199405.
13. Pickert G, Neufert C, Leppkes M, et al. STAT3 links IL-22 signaling in intestinal epithelial cells to mucosal wound healing. *J Exp Med.* 2009;206(7):1465-1472.

14. Divine JK, Staloch LJ, Haveri H, et al. GATA-4, GATA-5, and GATA-6 activate the rat liver fatty acid binding protein gene in concert with HNF-1alpha. *Am J Physiol Gastrointest Liver Physiol.* 2004;287(5):G1086-G1099.
15. Van der Sluis M, De Koning BA, De Bruijn AC, et al. Muc2-deficient mice spontaneously develop colitis, indicating that MUC2 is critical for colonic protection. *Gastroenterology.* 2006;131(1):117-129.
16. Takeichi M. Cadherin cell adhesion receptors as a morphogenetic regulator. *Science.* 1991;251(5000):1451-1455.
17. Shaikh M, Rajan K, Forsyth CB, Voigt RM, Keshavarzian A. Simultaneous gas-chromatographic urinary measurement of sugar probes to assess intestinal permeability: use of time course analysis to optimize its use to assess regional gut permeability. *Clin Chim Acta.* 2015;442:24-32.
18. Parks DH, Chuvochina M, Reeves PR, Beatson SA, Hugenholtz P. Reclassification of Shigella species as later heterotypic synonyms of Escherichia coli in the Genome Taxonomy Database. *bioRxiv* doi:10.1101/2021.09.22.461432
19. Parsons MJ, Moffitt TE, Gregory AM, et al. Social jetlag, obesity and metabolic disorder: investigation in a cohort study. *Int J Obes (Lond).* 2015;39(5):842-848.
20. Chakradeo PS, Keshavarzian A, Singh S, et al. Chronotype, social jet lag, sleep debt and food timing in inflammatory bowel disease. *Sleep Med.* 2018;52:188-195.
21. Forsyth CB, Shaikh M, Bishehsari F, et al. Alcohol feeding in mice promotes colonic hyperpermeability and changes in colonic organoid stem cell fate. *Alcohol Clin Exp Res.* 2017;41(12):2100-2113.
22. Summa KC, Voigt RM, Forsyth CB, et al. Disruption of the circadian clock in mice increases intestinal permeability and promotes alcohol-induced hepatic pathology and inflammation. *PLoS One.* 2013;8(6):e67102.
23. Oh SK, Kim D, Kim K, et al. RORalpha is crucial for attenuated inflammatory response to maintain intestinal homeostasis. *Proc Natl Acad Sci U S A.* 2019;116(42):21140-21149.
24. Babickova J, Tothova L, Lengyelova E, et al. Sex differences in experimentally induced colitis in mice: a role for estrogens. *Inflammation.* 2015;38(5):1996-2006.
25. Ortona E, Pierdominici M, Rider V. Editorial: sex hormones and gender differences in immune responses. *Front Immunol.* 2019;10:1076.
26. Qian J, Morris CJ, Caputo R, Wang W, Garaulet M, Scheer F. Sex differences in the circadian misalignment effects on energy regulation. *Proc Natl Acad Sci U S A.* 2019;116(47):23806-23812.
27. Santhi N, Lazar AS, McCabe PJ, Lo JC, Groeger JA, Dijk DJ. Sex differences in the circadian regulation of sleep and waking cognition in humans. *Proc Natl Acad Sci U S A.* 2016;113(19):E2730-E2739.
28. Amasheh S, Meiri N, Gitter AH, et al. Claudin-2 expression induces cation-selective channels in tight junctions of epithelial cells. *J Cell Sci.* 2002;115(Pt 24):4969-4976.
29. Kuo WT, Zuo L, Odenwald MA, et al. The tight junction protein ZO-1 is dispensable for barrier function but critical for effective mucosal repair. *Gastroenterology.* 2021;161(6):1924-1939.
30. Kyoko OO, Kono H, Ishimaru K, et al. Expressions of tight junction proteins Occludin and Claudin-1 are under the circadian control in the mouse large intestine: implications in intestinal permeability and susceptibility to colitis. *PLoS One.* 2014;9(5):e98016.
31. Sugimoto K. Role of STAT3 in inflammatory bowel disease. *World J Gastroenterol.* 2008;14(33):5110-5114.
32. Musso A, Dentelli P, Carlino A, et al. Signal transducers and activators of transcription 3 signaling pathway: an essential mediator of inflammatory bowel disease and other forms of intestinal inflammation. *Inflamm Bowel Dis.* 2005;11(2):91-98.
33. Bromberg J, Wang TC. Inflammation and cancer: IL-6 and STAT3 complete the link. *Cancer Cell.* 2009;15(2):79-80.
34. Wang Y, Mumm JB, Herbst R, Kolbeck R, Wang Y. IL-22 increases permeability of intestinal epithelial tight junctions by enhancing Claudin-2 expression. *J Immunol.* 2017;199(9):3316-3325.
35. Xiong H, Hong J, Du W, et al. Roles of STAT3 and ZEB1 proteins in E-cadherin down-regulation and human colorectal cancer epithelial-mesenchymal transition. *J Biol Chem.* 2012;287(8):5819-5832.
36. Li DP, Cui M, Tan F, Liu XY, Yao P. High red meat intake exacerbates dextran sulfate-induced colitis by altering gut microbiota in mice. *Front Nutr.* 2021;8:646819.
37. Swanson GR, Gorenz A, Shaikh M, et al. Night workers with circadian misalignment are susceptible to alcohol-induced intestinal hyperpermeability with social drinking. *Am J Physiol Gastrointest Liver Physiol.* 2016;311(1):G192-G201.
38. Sokol H, Seksik P, Furet JP, et al. Low counts of Faecalibacterium prausnitzii in colitis microbiota. *Inflamm Bowel Dis.* 2009;15(8):1183-1189.
39. Mukherji A, Kobiita A, Ye T, Chambon P. Homeostasis in intestinal epithelium is orchestrated by the circadian clock and microbiota cues transduced by TLRs. *Cell.* 2013;153(4):812-827.
40. Swanson G, Forsyth CB, Tang Y, et al. Role of intestinal circadian genes in alcohol-induced gut leakiness. *Alcohol Clin Exp Res.* 2011;35(7):1305-1314.
41. Xie G, Zhong W, Zheng X, et al. Chronic ethanol consumption alters mammalian gastrointestinal content metabolites. *J Proteome Res.* 2013;12(7):3297-3306.
42. Norman JM, Handley SA, Baldridge MT, et al. Disease-specific alterations in the enteric virome in inflammatory bowel disease. *Cell.* 2015;160(3):447-460.
43. Yu LC, Wei SC, Li YH, et al. Invasive pathobionts contribute to colon cancer initiation by counterbalancing epithelial antimicrobial responses. *Cell Mol Gastroenterol Hepatol.* 2022;13(1):57-79.
44. Viladomiu M, Metz ML, Lima SF, et al. Adherent-invasive E. coli metabolism of propanediol in Crohn's disease regulates phagocytes to drive intestinal inflammation. *Cell Host Microbe.* 2021;29(4):607-619.e8.
45. Clayburgh DR, Rosen S, Witkowski ED, et al. A differentiation-dependent splice variant of myosin light chain kinase, MLCK1, regulates epithelial tight junction permeability. *J Biol Chem.* 2004;279(53):55506-55513.
46. Pai YC, Weng LT, Wei SC, et al. Gut microbial transcytosis induced by tumor necrosis factor-like 1A-dependent activation of a myosin light chain kinase splice variant contributes to IBD. *J Crohns Colitis.* 2020;15(2):258-272.
47. Wei SC, Yang-Yen HF, Tsao PN, et al. SHANK3 regulates intestinal barrier function through modulating ZO-1 expression through the PKCepsilon-dependent pathway. *Inflamm Bowel Dis.* 2017;23(10):1730-1740.